INTERNATIONAL JOURNAL OF MARITIME TECHNOLOGY
IJMT Vol.2/ Summer 2014 (55-65)
Available online at: http://ijmt.ir/browse.php?a_code=A-10-93-1&sid=1&slc_lang=en

Estimation of Reshaped Profile of Berm Breakwaters Using Experimental Data

Alireza Sadat Hosseini[1], Mehdi Shafieefar[2]

[1] *M.Sc.; Faculty of Civil and Environmental Engineering, Tarbiat Modares University, Tehran; a.sadat@modares.ac.ir*
[2] *Professor; Faculty of Civil and Environmental Engineering, Tarbiat Modares University, Tehran; shafiee@modares.ac.ir*

ARTICLE INFO

Article History:
Received: 8 Apr. 2014
Accepted: 4 Aug. 2014
Available online: 22 Sep. 2014

Keywords:
Berm breakwater
Seaward profile
Reshaping parameters
M5' model tree
Computer program

ABSTRACT

A reshaping berm breakwater is a type of rubble mound breakwater in which, its seaward slope is allowed to reshape under wave attacks. There are some key parameters in the reshaped seaward profiles, which can schematize the reshaped profile of a berm breakwater. A total of 412 test results was used directly to cover the impact of sea state conditions and structural parameters on these reshaping parameters. In this study, the key parameters are derived using the M5' model trees. According to these new reshaping parameters, a computer program is written in MATLAB to predict the reshaped profile of a berm breakwater. The performance of the new program is compared with BREAKWAT software in the range of variation of the experimental data.

1. Introduction

The main design idea of berm breakwaters is that they should be built of two stone classes with a wide size gradation, allowing a considerable reduction of armor stone size. These structures are allowed to reshape, with stones moving up and down the slope, into a S-shape profile, which is assumed to be a more stable profile and the structures are sometimes referred to as dynamically stable structures [1].

Estimation of seaward reshaped profile of berm breakwaters is considered in this research by presenting a new method based on fundamental parameters related to this profile. Some of these parameters are investigated in previous studies. For instance, the recession (*Rec*) parameter [2-10]. The other parameters like depth of interception of reshaped and initial profiles (h_f) [11]. the lower step height (h_s) [6,12]. The upper step height (h_t) [13]. The other parameters, by which the reshaped profile of a berm breakwater could be parameterized, are the lower linear part (*Cot* α_{dd}) and upper linear part (*Cot* α_{du}) slope of reshaped profile and the lower part protrusion (ΔR). These parameters are illustrated in Figure 1. Thus, by means of these geometrical parameters the reshaped profile can be estimated.

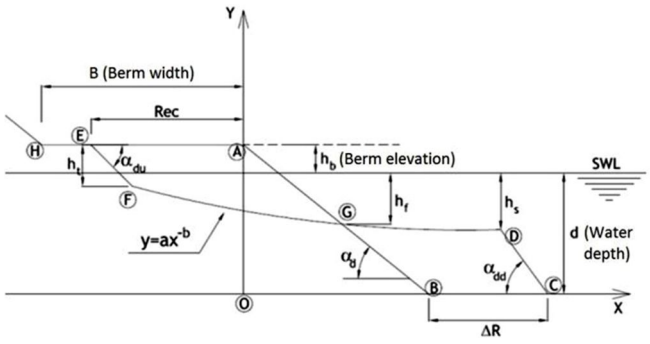

Figure 1. Reshaped profile and its fundamental geometrical parameters

The prediction of the reshaped profile of slopes in coastal area by means of physical modeling was investigated [14]. The stability of reshaping profile in rubble mound breakwaters with rock or concrete cube armors was studied [15]. the first version of his computer software, named "BREAKWAT" was released [16], in order to predict the reshaped profile in berm breakwaters. According to the studies performed [6], Van der Meer method predicts the reshaped profile of dynamically stable berm breakwaters (H_0T_0>70) with acceptable accuracy. However, for statically stable berm breakwaters (H_0T_0>70) "BREAKWAT" software predicts overestimated damage for the breakwater. Besides, the cross-section area of eroded and accumulated parts are supposed to be equivalent in this method, while according to the experimental results, these two areas are not necessarily equal because of the material

[Downloaded from ijmt.ir on 2026-09-14]

compression phenomenon. A computer software named "IB" in which the reshaped profile of a rubble mound structure could be estimated, using some formulae based on statistical models was presented [17].

2. Experimental data

A total number of 412 test results are used in the present study, which are obtained from the experiments carried out [19].

The ranges of these effective parameters covered in the tests are listed in Table 1. The material properties related to different armor and filter layers are listed in Table 2.

Table 1. Ranges of dimensional and non-dimensional parameters

Parameter		Range
Wave height	H_s (m)	0.043 ~ 0.12
Peak wave period	T_p (s)	1 ~ 1.98
Water depth at the toe of the structure	d (m)	0.20 ~ 0.28
Berm width	B (m)	0.3 ~ 0.5
Berm elevation above SWL	h_b (m)	0.010 ~ 0.45
Front slope below berm level	$Cot(\alpha_d)$	1.25
Front slope above berm level	$Cot(\alpha_u)$	1.25
Rearward slope	$Cot(\alpha_r)$	1.25
Number of incident waves	N	500 ~ 6000
H_0		1.57 ~ 3.9
H_0T_0		31.6 ~ 143.9
$H_0\sqrt{T_0}$		6.3 ~ 24.4
S_{om}		0.013 ~ 0.121
R_e		Armor 1: 1.12×10^4 ~ 1.74×10^4 Armor 2: 1.53×10^4 ~ 2.27×10^4 Armor 3: 2.01×10^4 ~ 2.71×10^4

Table 2. Material properties in tests

		Armor 1	Armor 2	Armor 3	Filter
Shekari's experiments	ρ_s (Kg/m^3)	2700	2700	2700	2800
	W_{50} (Kg)	0.014	0.025	0.042	0.0014
	D_{50} (m)	0.017	0.021	0.025	0.007
	$f_g=D_{85}/D_{15}$	1.5	1.5	1.5	1.33
Moghim's experiments	ρ_s (Kg/m^3)	2600			2640
	W_{50} (Kg)	0.013			0.0013
	D_{50} (m)	0.017			0.0079
	$f_g=D_{85}/D_{15}$	1.5			1.33

3. Model tree

Model tree is one of the machine learning approaches which makes the complex configuration of some modeling subjects appear to be insoluble by dividing them into simpler subtasks.

The concept of M5' model tree algorithm is to build a local specialized linear regression model for each subspace of the initial whole model. The M5' Model tree was introduced [20] and it was expanded in the continue [21], which is called the M5' method. Some advantages are enumerated for model trees which make them convenient to be used as a regression method in performance analysis.

M5' models are built by a divide-and-conquer method. M5' model tree algorithm splitting criterion is based on reduction in measured standard deviation of the class values that reaches a node. The standard deviation reduction (SDR) is:

$$SDR = sd(T) - \sum_i \frac{|T_i|}{|T|} \times sd(T_i) \qquad (1)$$

In eq. (1), T is the representative of each set of examples reaches a specific node; T_i is the subset of examples that have the ith outcome of the potential set; and sd is the standard deviation.

Over elaborate structures are often produced in the division process by standard deviation reduction, so the pruning process will become necessary for the tree. Pruning method uses the expected estimated error of each node for each experimental data [21] After the pruning procedure, some discontinuities will be appeared in the neighboring leaves of the pruned tree. Thus, a smoothing procedure is necessary [20]. According to the experiments carried out [21], smoothing substantially increases the accuracy of predictions [22].

4. Governing Equations for Reshaping Parameters

During the investigations on reshaped profiles from existing data and according to other studies on reshaping profiles [13], it is concluded that, in under water part of the reshaped profile, the power function in form of $y=ax^{-b}$ fits properly to the experimental data. In addition, according to the existing data, it is observed that the reshaped profile shape is approximately in a linear form with constant slope near to the berm and the bottom. Accordingly, the main assumption of this study is that the reshaped profile consists of three parts; two linear parts in upper and lower sector and a curve with power function in the middle.

So, in this part, by means of M5' model tree, the fundamental reshaping parameters formulae, are derived.

In this study, M5' model was used to predict the recession parameter using data sets related to Moghim and Shekari experimental studies [18,19]. According to previous studies on recession, some important dimensionless parameters were used in order to cover the impact of sea state and structural parameters. These dimensionless parameters were examined to find the best relationship between themselves for predicting the goal parameters. Table 3 shows all the input parameters used in M5' models.

[Downloaded from ijmt.ir on 2026-09-14]

Table 3. Range of dimensionless parameters used in M5' algorithm as the *input* parameters

dimensionless parameter	Range
H_0	1.57 ~ 3.9
$H_0\sqrt{T_0}$	6.3 ~ 24.4
$N/3000$	0.167 ~ 2
h_b/D_{n50}	0.4 ~ 4.11
H_s/D_{n50}	2.12 ~ 6.65
h_b/H_s	0.1 ~ 1.17
d/D_{n50}	8.0 ~ 16.5
B/D_{n50}	12 ~ 26.5
B/d	1.25 ~ 2

To build the M5' model, the whole dataset was split into the training set and testing set randomly. Training set includes 70 percent of the whole data (288 data points) and the rest of the data (30%) was used as testing set (124 data points). The models were trained using the training set and then evaluated by the testing data. The new M5' models were compared with the prior models presented by researchers.

4.1. Front Slope Recession (*Rec*)

As Figure 1 shows, in order to find the point "E", the recession parameter should be estimated. According to the explanations given at the beginning of this part, a model tree is built to find an equation for recession (the MT1 model).

The results of MT1 are presented as eq. (2) and (3):

If $H_0\sqrt{T_0} \le 10.2$, then

$$\frac{\mathrm{Re}\,c}{D_{n50}} = 0.003\cdot\left(H_0\sqrt{T_0}\right)^{3.31}\cdot\exp\left[-0.12\cdot\left(\frac{B}{d}\right)\right]\cdot \left(\frac{d}{D_{n50}}\right)^{0.612}\left(\frac{B}{D_{n50}}\right)^{-0.341}\left(\frac{h_b}{D_{n50}}\right)^{-0.194}\left(\frac{N}{3000}\right)^{0.2} \quad (2)$$

and if $10.2 < H_0\sqrt{T_0}$, then

$$\frac{\mathrm{Re}\,c}{D_{n50}} = 0.208\cdot\left(H_0\sqrt{T_0}\right)^{1.26}\cdot\exp\left[0.376\cdot\left(\frac{B}{d}\right)\right]\cdot \left(\frac{d}{D_{n50}}\right)^{1.036}\left(\frac{B}{D_{n50}}\right)^{-0.77}\left(\frac{h_b}{D_{n50}}\right)^{-0.178}\left(\frac{N}{3000}\right)^{0.2} \quad (3)$$

In order to evaluate the performance of the new M5' model for its predictions, following statistical parameters (Eq. (4) to Eq. (7)) were used: correlation of coefficients (R^2), root mean square error (*RMSE*) and percentage of relative error (*E*) and index of model performance (d_r) [23], which is a reformulation of Willmott's index of agreement (IW) [24].

$$R^2 = \left(\frac{n\cdot\sum_1^n P\cdot O - \left(\sum_1^n P\right)\cdot\left(\sum_1^n O\right)}{\sqrt{\left(n\cdot\sum_1^n P^2 - \left(\sum_1^n P\right)^2\right)\left(n\cdot\sum_1^n O^2 - \left(\sum_1^n O\right)^2\right)}}\right)^2 \quad (4)$$

$$RMSE = \sqrt{\frac{\sum_1^n (O-P)^2}{n}} \quad (5)$$

$$E = \frac{100}{n}\cdot\sum_1^n\left|\frac{O-P}{O}\right| \quad (6)$$

$$d_r = \begin{cases} 1 - \dfrac{\sum_{i=1}^n |P_i - O_i|}{c\sum_{i=1}^n |O_i - \bar{O}|} & , \ \sum_{i=1}^n |P_i - O_i| \le c\sum_{i=1}^n |O_i - \bar{O}| \\ \dfrac{c\sum_{i=1}^n |O_i - \bar{O}|}{\sum_{i=1}^n |P_i - O_i|} - 1 & , \ \sum_{i=1}^n |P_i - O_i| > c\sum_{i=1}^n |O_i - \bar{O}| \end{cases} \quad (7)$$

where, P is the predicted value, O is the observation data and n is the total number of measurements.

Scatter diagrams of measured and predicted dimensionless recession by the model tree are shown in Figure 2 to 6. In order to make a proper comparison between the new models and the previous ones, the statistical parameters (R^2, *RMSE*, *E* and d_r) were calculated. These statistical parameters indicate that the correlation of predicted recession by the M5' model tree is more precise than prior empirical formulae [9,10]. Table 4 shows the validation indices between predicted and measured dimensionless recession for new formula in total data and that of two mentioned formulae.

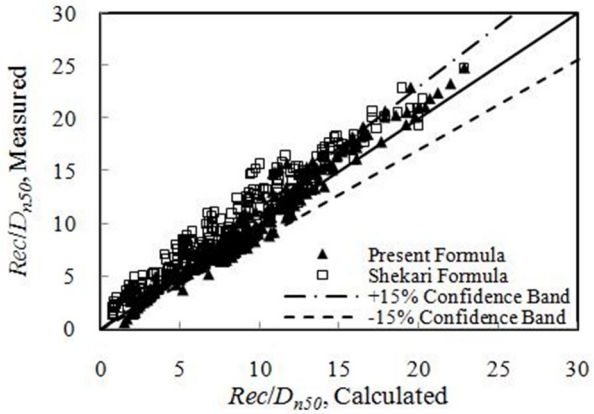

Figure 2. Measured and predicted dimensionless recession by MT1 compared to Shekari & Shafieefar formula [10] (Shekari dataset [19])

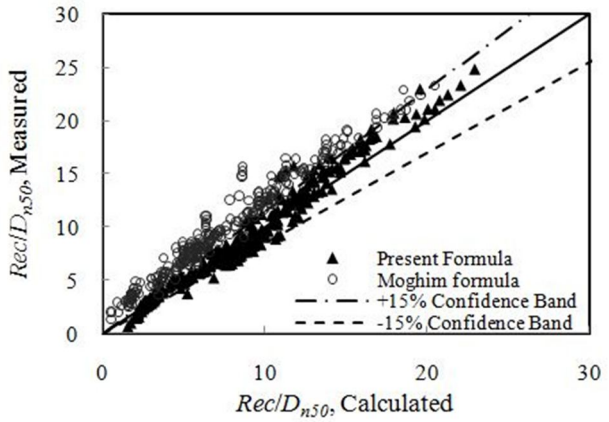

Figure 3. Measured and predicted dimensionless recession by MT1 compared to Moghim formula [9] (Shekari dataset [19])

[Downloaded from ijmt.ir on 2026-09-14]

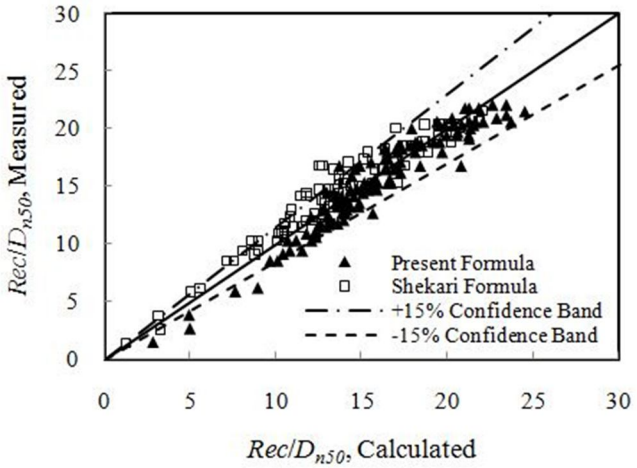

Figure 4. Measured and predicted dimensionless recession by MT1 compared to Shekari & Shafieefar formula [10] (Moghim dataset [18])

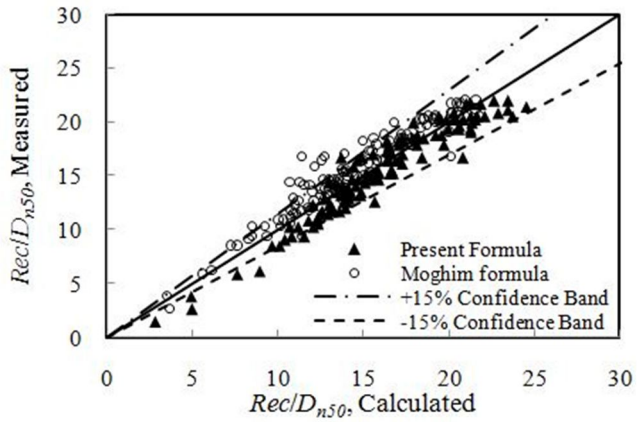

Figure 5. Measured and predicted dimensionless recession by MT1 compared to Moghim formula [9] (Moghim dataset [18])

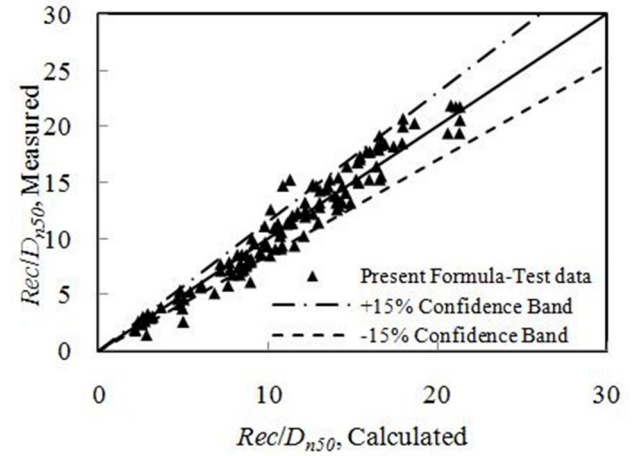

Figure 6. Measured and predicted dimensionless recession by MT1 in testing data

Table 4. Validation indices between predicted and measured dimensionless recession for new formula (total data) and 2 other formulae.

Experimantal data	Validation indices	Present Equations	Shekari & Shafieefar [11]	Moghim et al. [9]
Shekari data set	R^2	96%	92%	91%
	RMSE	0.97	1.02	1.09
	E	9.83%	17.88%	21.55%
	d_r	0.89	0.81	0.78
Moghim data set	R^2	93%	92%	92%
	RMSE	1.08	1.19	1.21
	E	7.65%	7.93%	8.29%
	d_r	0.85	0.73	0.82

4.2. Depth of interception of reshaped and initial profiles (h_f)

As it is presented in Figure 1, estimation of "h_f" parameter, helps find the point "G". Similar to the prior parameter, MT2 (The second model tree) is built and its result is as Eq. (7):

$$\frac{h_f}{D_{n50}} = 0.16 \cdot \left(\frac{d}{D_{n50}}\right)^{1.4} \cdot \left(\frac{h_b}{D_{n50}}\right)^{-0.26} \qquad (7)$$

According to Eq.(7), Depth of interception of reshaped and initial profiles depends on the water depth in front of the structure (d) and berm elevation (h_b).

Some researchers presented equations to estimate depth of intersection (h_f) [1,11]. Figure 7 illustrates the scatter diagram of calculated and measured dimensionless depth of intersection for Eq.(7) and the two mentioned equations. Figure 8 shows the scatter diagram of calculated and measured dimensionless depth of intersection for Eq.(7) in testing data. Table 5 shows the validation indices between predicted and measured dimensionless depth of intersection.

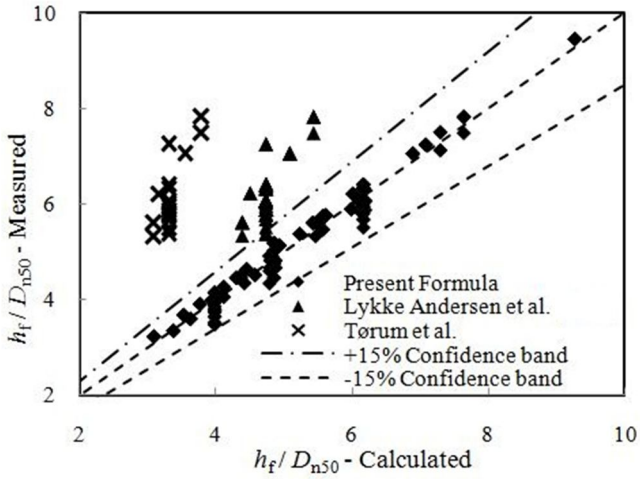

Figure 7. Comparing the measured and predicted dimensionless h_f by MT2 and 2 other formulae [11,5] in total data

[Downloaded from ijmt.ir on 2026-09-14]

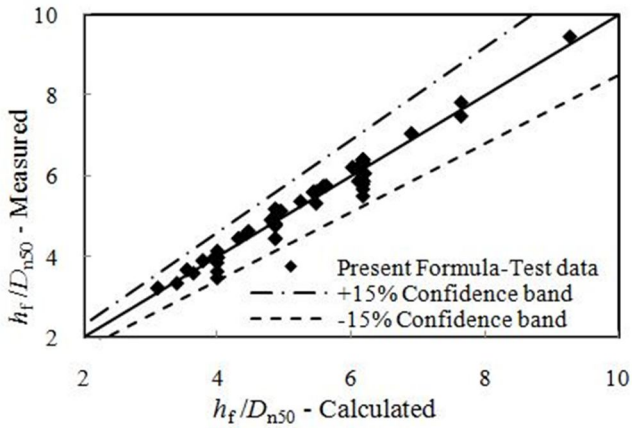

Figure 8. Measured and predicted dimensionless h_f by MT2 in testing data

Table 5. Validation indices between predicted and measured dimensionless h_f for new formula (total data) and 2 other formulae.

Validation indices	Present Equation	Lykke Andersen et al. [11]	Tørum et al. [5]
R^2	97.8%	66.1%	66.1%
RMSE	0.18	2.40	3.09
E	3.38%	18.94%	27.74%
d_r	0.86	0.62	0.49

4.3. Lower step height (h_s)

In order to find the point "D" from the reshaped profile, estimation of this parameter is necessary. In fact, this parameter characterizes the point where the slope in the lower part of reshaped profile changes. Eq.(8) shows the MT2 for prediction of lower step height (h_s).

$$\frac{h_s}{D_{n50}} = \left(H_0\sqrt{T_0}\right)^{0.47} \cdot \exp\left[0.58\left(\frac{B}{d}\right) - 0.39\right] \times \left(\frac{B}{D_{n50}}\right)^{-0.15} \left(\frac{B}{d}\right)^{-0.83} \left(\frac{H_s}{D_{n50}}\right)^{0.69} \left(\frac{N}{3000}\right)^{0.2} \quad (8)$$

Eq.(8) shows that, the lower step height is increased by increasing the wave height and period, number of waves and water depth in front of the structure.

Figure 9 shows the calculated and measured dimensionless lower step height for Eq.(8) and Figure 10 shows the one presented by Lykke Andersen et al. [8]. Table 6 demonstrates the validation indices between predicted and measured dimensionless lower step height.

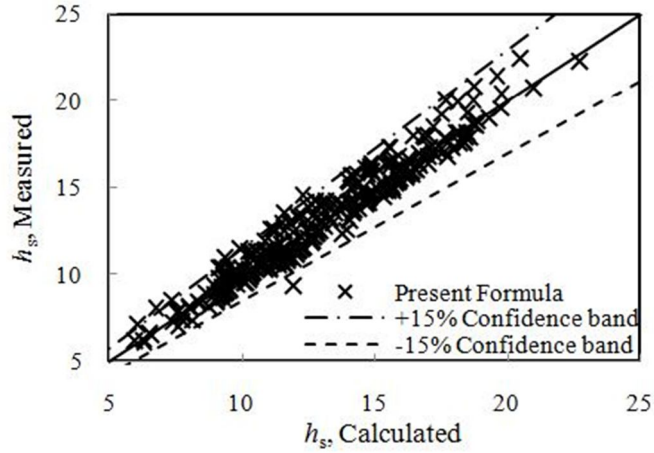

Figure 9. Comparing the measured and predicted dimensionless h_s by MT3 in total data

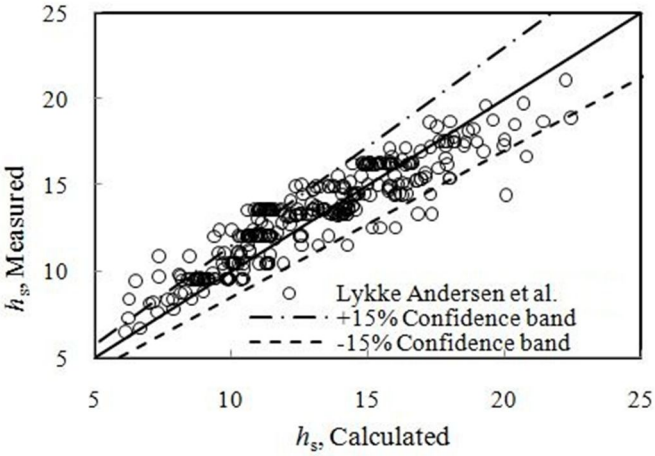

Figure 10. Comparing the measured and predicted dimensionless h_s by Lykke Andersen et al. equation [8] in total data

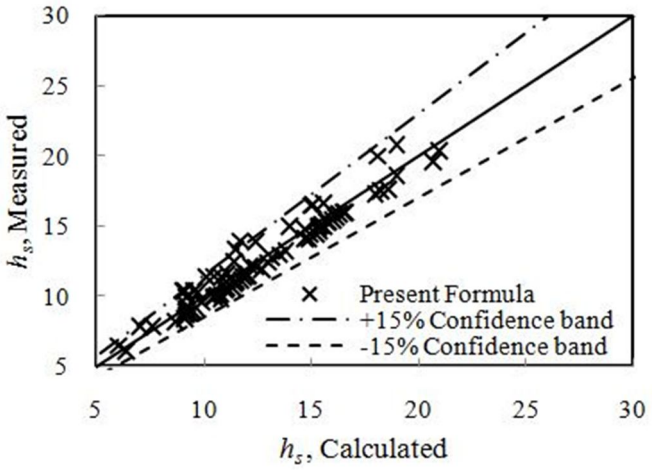

Figure 11. Measured and predicted dimensionless h_s by MT3 in testing data

Table 6. Validation indices between predicted and measured dimensionless h_s for new formula and the other one.

Validation indices	Present Equation	Lykke Andersen et al. [8]
R^2	94.2%	74.1%
RMSE	0.76	0.95
E	4.84%	6.72%
d_r	0.84	0.78

[Downloaded from ijmt.ir on 2026-09-14]

4.4. Upper step height (h_t)

The point "F" of reshaping profile (Figure 1) could be found when the upper step height is estimated. This parameter measures the depth of erosion in the upper part of reshaped profile.

MT4 is built to find the Eq.(9) in order to estimate the upper step height (h_t).

$$\frac{h_t}{D_{n50}} = 0.268\left(H_0\sqrt{T_0}\right)^{0.21}\left(\frac{d}{D_{n50}}\right)^{0.9}\left(\frac{h_b}{H_s}\right)^{0.3} \quad (9)$$

Eq.8 shows that, increasing wave period, water depth in front of the structure and berm elevation have an increasing effect on upper step height.

The comparisons between the experimental measurements and predictions of Eq.(9) may be found in Figure 12 and 13 and also in Table 7 quantitatively.

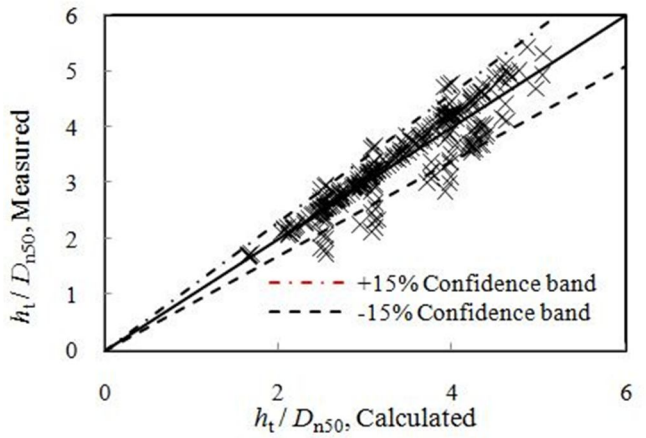

Figure 12. Comparing the measured and predicted dimensionless h_t by MT4 in total data

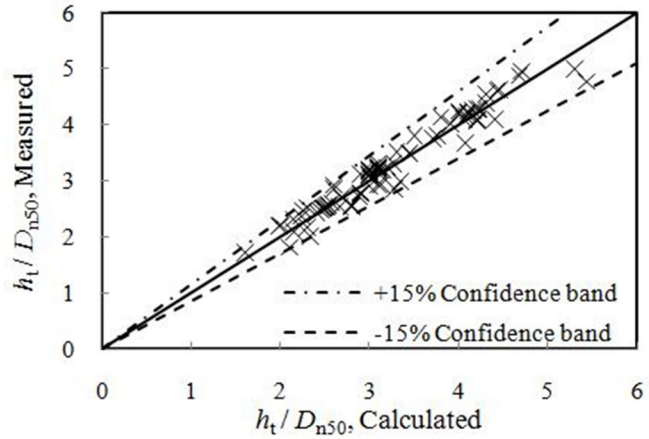

Figure 13. Measured and predicted dimensionless h_t by MT4 in testing data

Table 7. Validation indices between predicted and measured dimensionless h_t for Eq. (9).

Validation indices	Present Equation in total data	Present Equation in testing data
R^2	96.2%	93.0%
RMSE	0.11	0.18
E	1.54	3.09
d_r	0.89	0.83

4.5. Lower linear part slope (*Cot* α_{dd})

As it is explained in the introduction, in order to approximate the linear parts of the reshaped profile, it is needed to calculate the slope of these linear parts. For the lower part, in addition to lower step height (h_s), lower linear part slope (*Cot* α_{dd}) is schematized by MT5 as it is shown in Eq.(10).

$$Cot\alpha_{dd} = 0.065 \cdot H_0 + 1.33 \quad (10)$$

As it is obvious from Eq.(10), the lower linear part slope depends on H_0 (the stability parameter).

Similar to prior extracted equations for reshaping profile, measured and predicted *Cot* α_{dd} by MT5 is compared and illustrated in Figure 14 and 15. The validation indices are shown in Table 8.

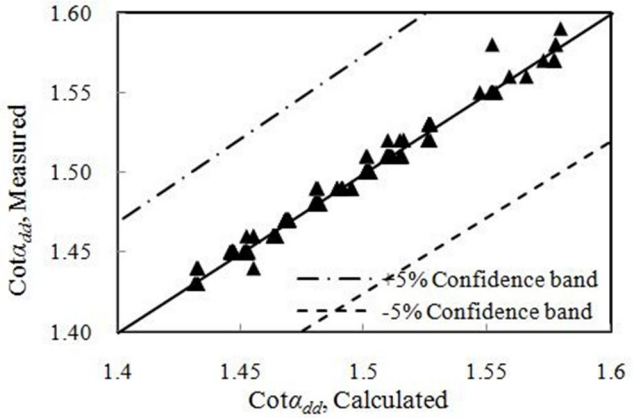

Figure 14. Comparing the measured and predicted *Cot* α_{dd} by MT5 in total data

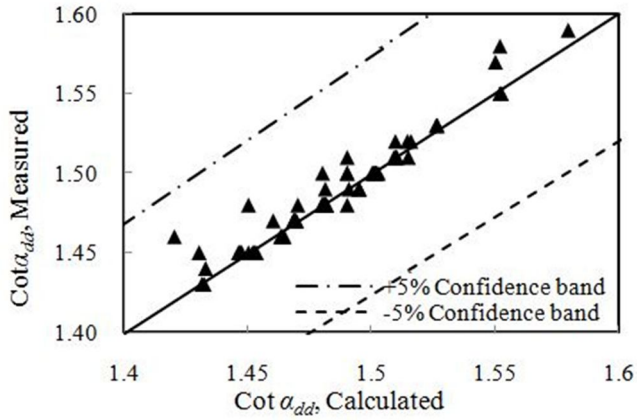

Figure 15. Measured and predicted *Cot* α_{dd} by MT5 in testing data

Table 8. Validation indices between predicted and measured Cotα_{dd} for Eq. (10)

Validation indices	Present Equation in total data	Present Equation in testing data
R^2	97.8%	93.9%
RMSE	0.035	0.084
E	0.21%	0.85%
d_r	0.93	0.89

[Downloaded from ijmt.ir on 2026-09-14]

4.6. Upper linear part slope ($Cot\ \alpha_{du}$)

Similar to the lower linear part, in order to draw the upper linear part, in addition to upper step height (h_t), lower linear part slope ($Cot\ \alpha_{du}$) must be estimated. To this aim, the MT6 eventuates in Eq.(11).

$$Cot\alpha_{du} = 0.062 \cdot H_0 + 1.265 \tag{11}$$

Figure 16 and 17 show the comparisons for the measured and predicted $Cot\ \alpha_{du}$ by MT6. Validation indices are presented in Table 9.

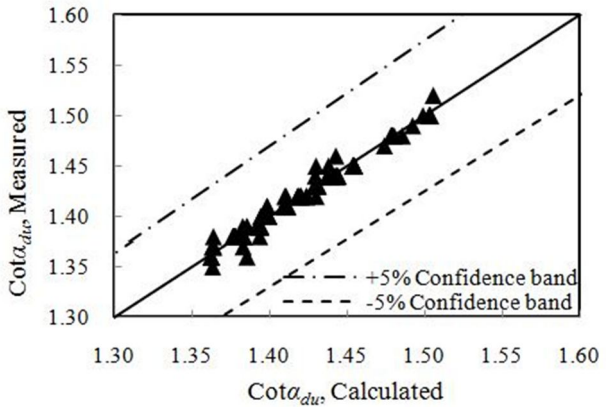

Figure 16. Comparing the measured and predicted $Cot\ \alpha_{du}$ by MT6 in total data

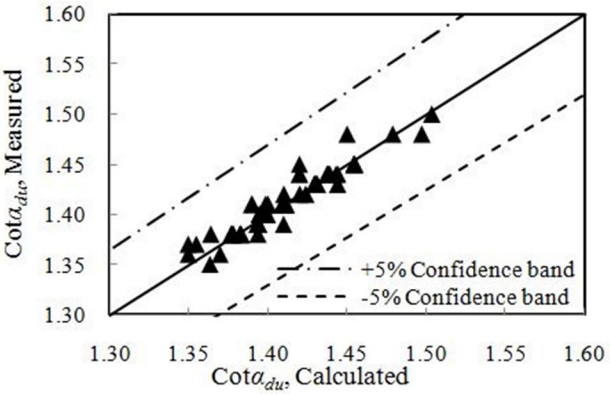

Figure 17. Measured and predicted $Cot\ \alpha_{dd}$ by MT5 in testing data

Table 9. Validation indices between predicted and measured $Cot\alpha_{du}$ for Eq. (11)

Validation indices	Present Equation in total data	Present Equation in testing data
R^2	97.2%	91.7%
RMSE	0.041	0.087
E	0.26	0.58
d_r	0.91	0.88

4.7. Lower part protrusility (ΔR)

This parameter is the last reshaping parameter which should be estimated. By means of Lower part protrusility (ΔR), point "C" may be specified. The MT7 is built to schematize this parameter as Eq.(12).

$$\Delta R = \left(H_0\sqrt{T_0}\right)^{1.167}\left(\frac{h_b}{D_{n50}}\right)^{-0.8}\left(\frac{d}{D_{n50}}\right)^{0.26}\left(\frac{N}{3000}\right)^{0.26} \times \exp\left[0.55\left(\frac{h_b}{D_{n50}}\right) - 0.18\left(\frac{B}{d}\right) - 1.54\right] \tag{12}$$

The measured and predicted ΔR by MT7 is compared and illustrated in Figure 18 and 19. The validation indices are shown in Table 10.

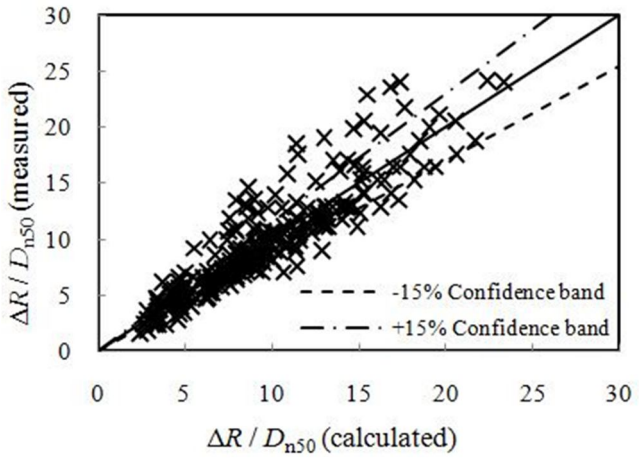

Figure 18. Comparing the measured and predicted ΔR by MT7 in total data

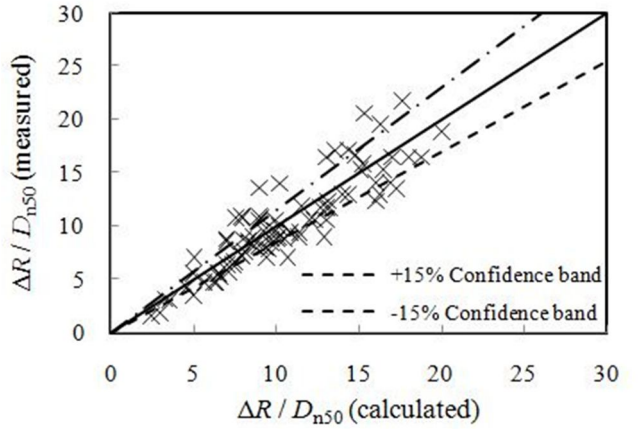

Figure 19. Measured and predicted ΔR by MT7 in testing data

Table 10. Validation indices between predicted and measured ΔR for Eq. (12)

Validation indices	Present Equation in total data	Present Equation in testing data
R^2	83.2%	80.8%
RMSE	1.93	2.10
E	12.27	16.13
d_r	0.79	0.76

It worth to be noted that, the final number of input parameters in every seven reshaping formulae, has been set after an optimization through the sensitivity analysis, which is hereafter briefly summarized as the *RMSE* variation percentage due to elimination of each parameter in Table 11.

[Downloaded from ijmt.ir on 2026-09-14]

Table 11. Sensivity analysis to different type of dimensionless input parameters for each output parameter. Numbers represent the percentage of *RMSE* variation due to elimination of each parameter

Eliminated parameter	Ln Rec/D_{n50}	Ln h_f/D_{n50}	Ln h_s/D_{n50}	Ln h_t/D_{n50}	cotα_{dd}	cotα_{du}	Ln $\Delta R/D_{n50}$
H_0	-16.4	-6.1	-0.5	-1.9	24.9	13.1	-2.5
H_0T_0	-0.4	-7.2	-0.8	-0.4	-2.7	-3.2	-0.2
$H_0\sqrt{T_0}$	2.3	-26.5	-0.4	-0.1	-1.0	-0.5	0.1
N/3000	-11.7	-21.1	-0.3	-12.9	-6.0	-7.6	-1.5
h_b/D_{n50}	-8.6	-0.7	-1.2	-10.0	-3.5	-36.9	4.4
H_s/D_{n50}	-6.3	-3.9	-5.8	-7.5	-17.7	-14.9	-7.2
d/D_{n50}	-6.9	-0.3	-2.6	-0.3	-2.3	-9.8	-3.2
B/D_{n50}	-14.4	-19.2	-4.8	-10.0	-19.6	-5.7	-1.6
h_b/H_s	-12.2	-25.2	-5.7	-3.4	-4.1	-15.2	-4.4
B/d	6.4	-15.2	2.8	-13.8	-26.8	-24.8	2.4
h_b/d	-8.4	-7.0	-7.7	-12.6	-12.6	-17.6	-13.1
h_b/B	-2.3	-28.2	-12.2	-2.5	-31.1	-18.4	-8.2
H_s/d	-11.0	-20.3	-8.9	-3.0	-18.5	-31.0	-7.2
H_s/B	-24.4	-27.4	-12.3	-13.7	-7.4	-36.9	-3.2
LnH_0	-18.3	-7.1	-15.0	-3.8	-9.1	-25.4	-0.7
LnH_0T_0	-12.1	-4.8	-15.8	-7.6	-24.7	-17.2	-0.2
$LnH_0\sqrt{T_0}$	22.3	-6.9	6.1	2.3	-23.7	-25.4	14.0
LnN/3000	7.2	-8.2	1.9	-0.3	-4.3	-18.4	3.2
Lnh_b/D_{n50}	12.6	8.6	-14.3	-0.1	-19.5	-17.2	3.6
LnH_s/D_{n50}	0.1	-9.2	0.4	-19.0	-35.2	-13.1	-15.6
Lnd/D_{n50}	38.6	15.4	-13.2	15.3	-23.7	-13.7	4.9
LnB/D_{n50}	33.6	-4.6	4.4	-11.4	-16.1	-18.1	-7.4
Lnh_b/H_s	-2.2	-7.1	-0.6	12.4	-16.0	-19.1	-1.6
LnB/d	-14.6	-2.1	0.4	-17.7	-16.3	-13.7	-2.5
Lnh_b/d	-17.4	-14.1	-22.9	0.1	-19.8	-21.6	-0.7
Lnh_b/B	-3.6	-16.4	-4.8	-10.0	-21.4	-25.0	-8.2
LnH_s/d	-4.8	-17.2	-9.8	-12.8	-21.6	-24.6	-0.8
LnH_s/B	-12.2	-7.2	-0.6	-15.2	-18.5	-13.3	-16.2

5. A computer program for prediction of reshaped profile

5.1. Program algorithm

In this part the algorithm of the computer program by which the reshaped profile of berm breakwaters could be predicted is explained. In this algorithm, the seven equations driven for fundamental reshaping parameters are used. In order to draw the initial profile of the berm breakwater, the input parameters of the algorithm are initial berm width, upper and lower part slope of breakwater with respect to berm elevation, water depth and berm elevation with respect to the still water level. The algorithm of drawing this initial profile by the program is as follow and also schematized in Figure 20:

1- According to Figure 20, it is supposed that the x axis is coincident with the sea bottom level and the y axis crosses from the slope changing point (Point "B"). The still water level equation is expressed as "$y=d$".

2- In order to draw the reshaped profile, having recession (*Rec*) parameter, we move from point "A" as "*Rec*" to the point "E".

3- From point "E", a line with slope of -$Cot\alpha_{du}$ is drawn to the point "F" with the Y coordinate of $d+h_b-h_t$.

4- Moving from point "B" as "ΔR" to the point "C".

5- From point "C", a line with slope of $Cot\alpha_{dd}$ is drawn to the point "D" with the Y coordinate of d -hs.

6- The point "G" with the Y coordinate of $d-h_f$ is specified on the line "AB" (the lower seaward initial slope).

Thus, five fundamental points of the reshaped profile ("E", "F", "C", "D" and "G") are characterized. According to the test results and prior explanations, a power function ($y=ax^{-b}$) fits on points "D", "G" and "F".

This new method for prediction of reshaped profile is usable for berm breakwaters with the limitations listed in Eq. (13), and consequently it can be mentioned that, this method is usable for berm breakwaters in which their berm elevation is higher than SWL (h_b>0). It must be also noted that, this method is applicable for high-crested berm breakwaters with low mean overtopping discharge.

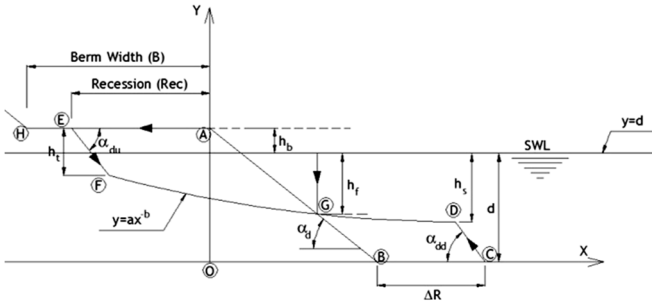

Figure 20. The process of drawing the reshaped profile according to program algorithm

5.2. Comparing the new program and BREAKWAT3 estimation of reshaped profile

In this part a comparison is made on some experimental results which can be found in Figure 21 to 28. In order to make a more comprehensive comparison, these tests are chosen with varied structural and sea state parameters among those profiles which are not used as training set in the modeling. The specifications of these tests are illustrated in Table 12.

Table 12. The specifications of various test results for comparison the new program and BREAKWAT3

Figure number	D_{n50} (cm)	d (cm)	H_s (cm)	T_p (s)
21, 22	1.7	24	7.45	1.27
23, 24	1.7	24	8.55	1.54
25, 26	1.7	26	6.55	1
27, 28	2.5	24	9.65	1.54
Figure number	B (cm)	N	h_b (cm)	
21, 22	35	3000	4	
23, 24	40	1000	4	
25, 26	40	3000	4	
27, 28	40	3000	5.5	

[Downloaded from ijmt.ir on 2026-09-14]

In following figures, measured and estimated reshaped profiles, which predicted by the program of this study and BREAKWAT3, are presented distinctively. It must be noted that, the axis units and also the *x*-axis zero point are different in each pair of figures.

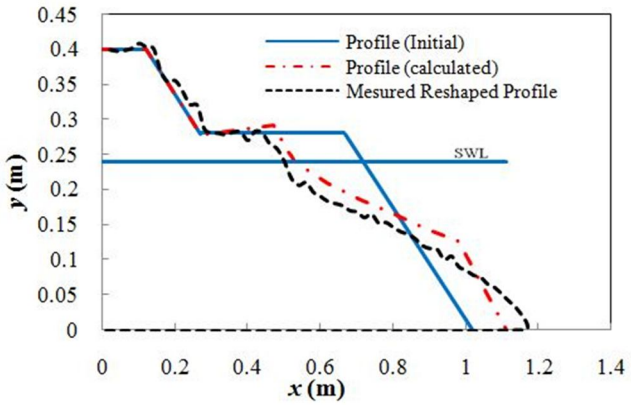

Figure 21. Measured and predicted reshaping profile by BREAKWAT3 in first raw of Table 11

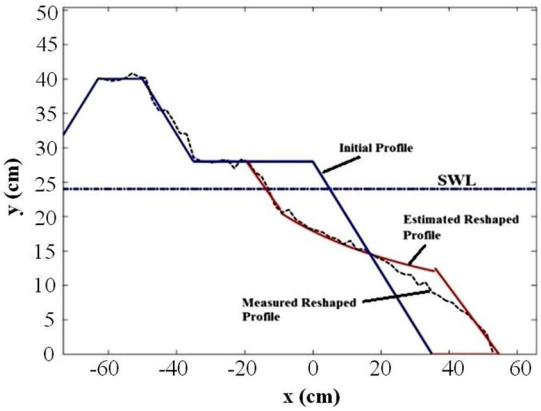

Figure 22. Measured and predicted reshaping profile by the new program of this study in first raw of Table 11

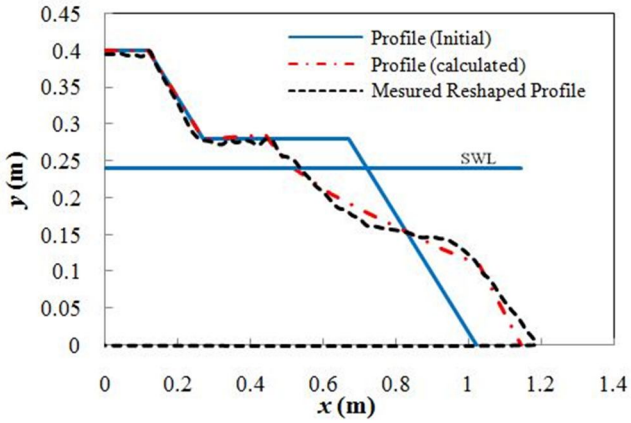

Figure 23. Measured and predicted reshaping profile by BREAKWAT3 in second raw of Table 11

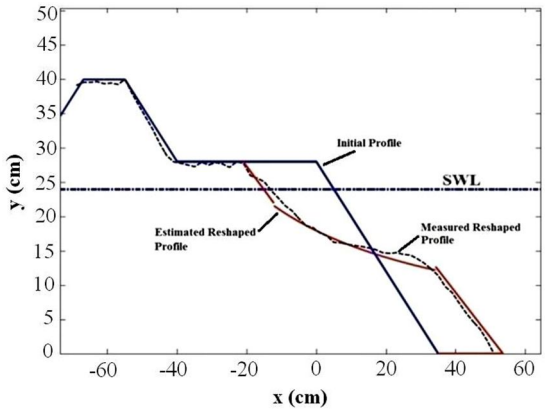

Figure 24. Measured and predicted reshaping profile by the new program of this study in second raw of Table 11

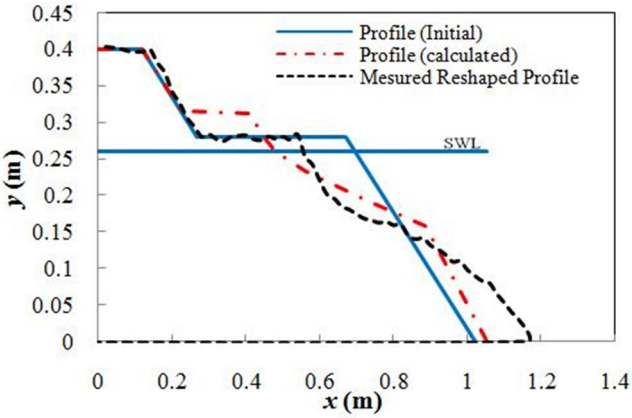

Figure 25. Measured and predicted reshaping profile by BREAKWAT3 in third raw of Table 11

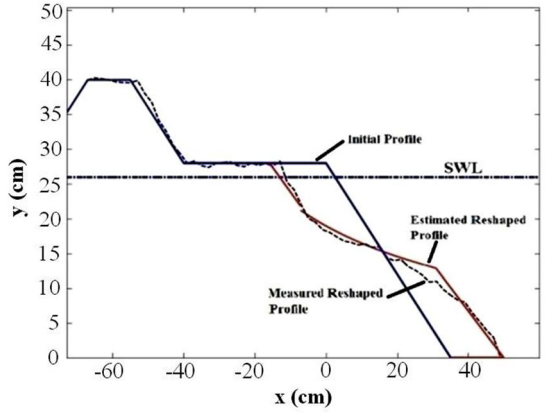

Figure 26. Measured and predicted reshaping profile by the new program of this study in third raw of Table 11

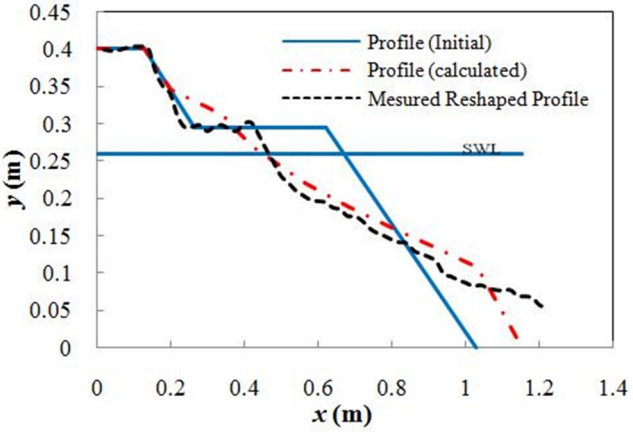

Figure 27. Measured and predicted reshaping profile by BREAKWAT3 in forth raw of Table 11

[Downloaded from ijmt.ir on 2026-09-14]

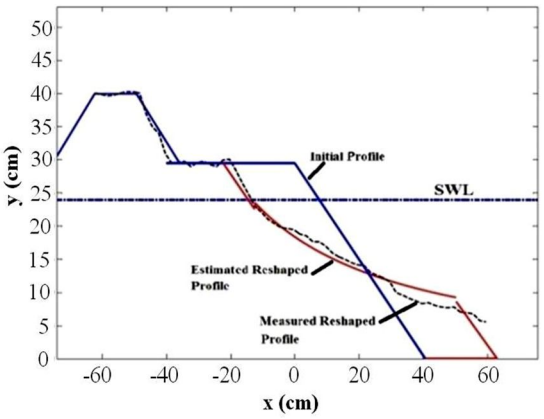

Figure 28. Measured and predicted reshaping profile by the new program of this study in forth raw of Table 11

According to Figures 21 to 28, the new proposed computer program shows more precise estimate of the reshaped profile in comparison to the BREAKWAT3. In order to make a quantitative comparison, the fundamental parameters which schematize the reshaped profiles, driven by the new program and BREAKWAT3, are compared with together two by two. Results of the relative percentage error for these estimations is given in Table 13.

Table 13. Comparison of relative percetage of error (E) between the new program and BREAKWAT3

Reshaping parameters	Figure number	*Rec*	h_f	h_s	h_t	Cotα_{dd}	Cotα_{du}	ΔR
The new program of this study	7, 8	1.20	4.0	14.0	1.6	45.5	2.2	13.4
	9, 10	0.60	13.3	22.2	26.7	9.0	4.2	0.0
	11, 12	25.0	9.5	11.1	17.3	16.4	3.6	5.7
	13, 14	12.5	12.5	5.7	12.0	53.1	2.2	21.4
BREAKWAT 3	7, 8	6.60	13.1	16.3	57.6	55.5	8.3	45.3
	9, 10	17.1	43.3	16.3	47.2	13.4	11.5	50.6
	11, 12	81.0	27.3	30.9	69.8	42.5	14.1	72.8
	13, 14	49.4	16.7	2.5	62.3	60.0	26.8	14.7

6. Conclusions

In this study, seven new formulae for seven fundamental reshaping parameters are presented which were driven using M5' machine learning approach on data of 412 tests. By means of these seven formulae, a geometric algorithm is written in a computer program which could predict the reshaped profile in seaward slope of berm breakwater. The following results can be drawn from the present study:

- The predictive accuracy of the model trees, was observed to be high enough in the estimation of the equations for reshaping parameters.
- According to presented results, the introduced new program shows better results for validation indices comparing to those of BREAKWAT3 in the range of parameters governed by the existing datasets.

7. References

1- PIANC, (2003). *State-of-the-Art of Designing and Constructing Berm Breakwaters*. WG40.

2- Hall, K. and Kao, S., (1991). *A Study of the Stability of Dynamically Stable Breakwaters.* Canadian Journal of Civil Engineering, Vol. 18, pp.916-925.

3- Tørum, A., (1998). *On the Stability of Berm Breakwaters in Shallow and Deep Water*. Proc. Of the 26th International Conference on Coastal Engineering, Copenhagen, Denmark, ASCE.

4- Lissev, N. and Daskalov, K., (2000). *Berm Type Breakwater – an Alternative Solution for New East Breakwater for Port of Burgas.* Report No. R-8-93, Department of Structural Engineering, University of Trondheim, The Norwegian Institute of Technology.

5- Tørum, A., Kuhnen, F., Menze, A., (2003). *On Berm Breakwaters. Stability, Scour, Overtopping.* Elsevier, Journal of Coastal Engineering 49, Amsterdam, September Issue, pp. 209-238.

6- Lykke Andersen, T., (2006). *Hydraulic Response of Rubble Mound Breakwaters (Scale Effects - Berm Breakwaters)*. Doctoral Thesis, University of Aalborg, Denmark, Under Supervision of Burcharth, H. F.

7- Sigurdarson, S., Van der Meer, J.W., Burcharth, H.F., and Sørensen, J.D., (2007). *Optimum safety levels and design rules for the Icelandic-type berm breakwater*. Coastal structures conf., Venice.

8- Lykke Andersen, T., Burcharth, H.F., (2010). *A new formula for front slope recession of berm breakwaters*. Elsevier. Journal of Coastal Engineering 57, pp. 359–374.

9- Moghim, M.N., Shafieefar, M., Tørum, A. and Chegini, V., (2011). *A new formula for the sea state and structural parameters influencing the stability of homogeneous reshaping berm breakwaters.* Elsevier, Journal of Coastal Engineering 58, pp. 706-721.

10- Shekari, MR, Shafieefar, M., (2013). *An experimental study on the reshaping of berm breakwaters under irregular wave attacks*. Applied Ocean Research 42, 16–23.

11- Lykke Andersen, T., Van der Meer, J.W., Burcharth, H.F. and Sigurdarson, S., (2012). *Stability Of Hardly Reshaping Berm Breakwaters*. Proceedings of 33rd Conference on Coastal Engineering, Santander, Spain.

12- Van der Meer, J.W., (1988). *Rock Slopes and Gravel Beaches under Wave Attack*. Doctoral Thesis, Delft University of Technology, Also: Delft Hydraulics Communication, No.396.

13- Van der Meer, J.W., (1992). *Stability of seaward slope of berm breakwaters*. Coastal Engineering 16, 205–234.

14- Popov, I.J., (1960). *Experimental Research on Formation by Waves of Stable Profiles of Upstream Faces of Earth Dams and Reservoir Shores.* 7th Int. Conf. On Coastal Engineering, The Hague, PP 282-293.

15- Priest, M.S., Pugh, J.E., and Singh. R., (1964). *Seaward Profile for Rubble Mound Breakwaters*. 7th

[Downloaded from ijmt.ir on 2026-09-14]

Int. Conf. On Coastal Engineering, Lisbon, pp. 553-559.
16- BREAKWAT 3.0.22., (2003). *A commercial Software*, WL|Delft Hydraulics, in collaboration with the Delft University of Technology.
17- Ezabad, P, Shafieefar, M, Shirian, N., (2005). *Study of hydraulic stability of reshaping breakwaters based on experimental results*. International Journal Of Maritime Technology, (In Persian).
18- Moghim, MN., (2009). *Experimental study of hydraulic stability of reshaping berm breakwaters*. PhD thesis, Tarbiat Modares University.
19- Shekari, MR., (2013). *Experimental investigation of hydraulic stability of single berm and double berm breakwaters*. PhD thesis, Tarbiat Modares University.
20- Quinlan, J.R., (1992). *Learning with continuous classes*, Proc. of the 5th Australian Joint Conference on AI, 343-348.
21- Wang, Y., Witten, I., (1997). *Induction of model trees for predicting continuous classes*, Proc. of the Poster Papers of the ECML, 128-137.
22- Zhang D, Tsai JJP., (2007). *Advances in Machine Learning Applications in Software Engineering*, Idea Group Inc.
23- Willmott, C.J., Robeson, S.M., Matsuura, K., (2012). S*hort Communication A refined index of model performance*. International Journal of Climatology 32, 2088–2094.
24- Willmott, C.J., (1981). *On the validation of models*. Physical Geography 2: 184–194.

[Downloaded from ijmt.ir on 2026-09-14]